Oxygen Hydration Mechanism for the Oxygen Reduction Reaction at Pt and Pd Fuel Cell Catalysts

ARTICLE *in* JOURNAL OF PHYSICAL CHEMISTRY LETTERS · FEBRUARY 2011

Impact Factor: 7.46 · DOI: 10.1021/jz101753e

THE JOURNAL OF PHYSICAL CHEMISTRY Letters

LETTER

pubs.acs.org/JPCL

Oxygen Hydration Mechanism for the Oxygen Reduction Reaction at Pt and Pd Fuel Cell Catalysts

Yao Sha,[†] Ted H. Yu,[†] Boris V. Merinov,[†] Pezhman Shirvanian,[§] and William A. Goddard, III*[,†]

[†]Materials and Process Simulation Center, California Institute of Technology, MC 139-74, Pasadena, California 91125, United States

[§]Ford Motor Company, Research & Advanced Engineering, 2101 Village Rd, Dearborn, Michigan 48104, United States

Supporting Information

ABSTRACT: We report the reaction pathways and barriers for the oxygen reduction reaction (ORR) on platinum, both for gas phase and in solution, based on quantum mechanics calculations (PBE-DFT) on semi-infinite slabs. We find a new mechanism in solution: $O_2 \rightarrow 2O_{ad}$ (E_{act} = 0.00 eV), $O_{ad} + H_2O_{ad} \rightarrow 2OH_{ad}$ (E_{act} = 0.50 eV), $OH_{ad} + H_{ad} \rightarrow H_2O_{ad}$ (E_{act} = 0.24 eV), in which OH_{ad} is formed by the hydration of surface O_{ad}. For the gas phase (hydrophilic phase of Nafion), we find that the favored step for activation of the O_2 is $H_{ad} + O_{2ad} \rightarrow HOO_{ad}$ (E_{act} = 0.30 eV) $\rightarrow HO_{ad} + O_{ad}$ (E_{act} = 0.12 eV) followed by $O_{ad} + H_2O_{ad} \rightarrow 2OH_{ad}$ (E_{act} = 0.23 eV), $OH_{ad} + H_{ad} \rightarrow H_2O_{ad}$ (E_{act} = 0.14 eV). This suggests that to improve the efficiency of ORR catalysts, we should focus on decreasing the barrier for O_{ad} hydration while providing hydrophobic conditions for the OH and H_2O formation steps.

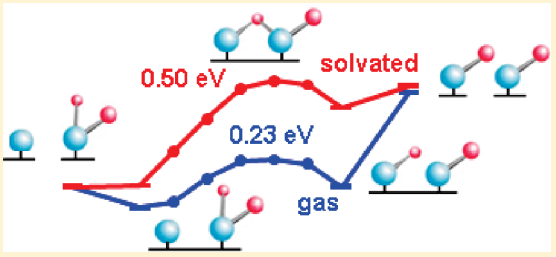

SECTION: Surfaces, Interfaces, Catalysis

Critical to the performance of polymer electrolyte membrane fuel cells (PEMFCs) is the efficiency of the reaction in which protons (passed through the electrolyte) from the anode reduce O_2 at the cathode to form H_2O, the oxygen reduction reaction (ORR).[1−4] Currently the best cathode catalysts are Pt or alloys of Pt with Co or Ni,[5,6] but the efficiency remains unacceptably low while the costs are too high. In order to improve the performance of current PEMFCs, it is important to understand the chemical mechanism, that is, the sequence of fundamental reaction steps taking protons delivered to the cathode and O_2 to form H_2O.

We consider here the Nafion PEMFC, in which we have shown[7,8] that for standard humidity conditions (H_2O/SO_3 ratio ∼15) the Nafion has percolating water channels (∼4 nm wide) with ionized sulfonic acid groups ($R-SO_3^-$) lining the surface intermixed with percolating hydrophobic (Teflon-like) regions (Figure 1). We assume here that O_2 accesses the catalyst surface via the hydrophobic regions (modeled as gas phase), while the protons migrate through the water channels (the solution phase).

The most common mechanism, denoted as **O_2-diss-gas**[9] is

$$O_{2g} \rightarrow O_{2ad} \quad \text{(no barrier)} \tag{1a}$$

$$O_{2ad} \rightarrow 2O_{ad} \quad [E_{act} = 0.57 \text{ eV (Pt)}, 0.72 \text{ (Pd)}] \tag{1b}$$

$$O_{ad} + H_{ad} \rightarrow OH_{ad} \quad [E_{act} = 0.74 \text{ eV (Pt)}, 0.30 \text{ (Pd)}] \tag{1c}$$

$$OH_{ad} + H_{ad} \rightarrow H_2O_{ad} \quad [E_{act} = 0.14 \text{ eV (Pt)}, 0.58 \text{ (Pd)}] \tag{1d}$$

Many studies have focused only on the O_2 dissociation step (step 1b),[10−13] however, we find step 1c to be the rate-determining step (RDS). Enthalpies and barriers for steps possibly important for ORR on Pt and Pd are presented in Table 1. Recently Mavrikakis et al.[14] published gas phase barriers for the first five reactions in Table 1a for Pt and Pd, but without allowing the metal surface slab to relax. As a result, their barriers are 0.00−0.25 eV too high for Pt and 0.00−0.65 eV too high for Pd.

A second possible pathway,[9] **HOO-form-gas**, for ORR involves activation of O_{2ad} with H_{ad} prior to dissociation:

$$O_{2g} \rightarrow O_{2ad} \quad \text{(no barrier)} \tag{2a}$$

$$H_{ad} + O_{2ad} \rightarrow HOO_{ad} \quad [E_{act} = 0.30 \text{ eV (Pt)}, 0.55 \text{ (Pd)}] \tag{2b}$$

$$HOO_{ad} \rightarrow HO_{ad} + O_{ad} \quad [E_{act} = 0.12 \text{ eV (Pt)}, 0.26 \text{ (Pd)}] \tag{2c}$$

$$O_{ad} + H_{ad} \rightarrow HO_{ad} \quad [E_{act} = 0.74 \text{ eV (Pt)}, 0.30 \text{ (Pd)}] \tag{2d}$$

$$OH_{ad} + H_{ad} \rightarrow H_2O_{ad} \quad [E_{act} = 0.14 \text{ eV (Pt)}, 0.58 \text{ (Pd)}] \tag{2e}$$

In this mechanism H_{ad} activates O_2 to form HOO (E_{act} = 0.30 eV), and then HOO_{ad} dissociates to form O_{ad} and OH_{ad} (E_{act} = 0.12 eV). This leads to a barrier of 0.30 eV, making the HOO pathway preferred over the direct O_2 dissociation pathway (0.57 eV) in the gas phase. However, the RDS remains step 2d (same as step 1c) (Table 1).

Received: December 31, 2010
Accepted: February 8, 2011
Published: February 24, 2011

   dx.doi.org/10.1021/jz101753e | J. Phys. Chem. Lett. 2011, 2, 572–576

In the above mechanisms, H_{ad} is assumed to be available as a reactant on the surface. At normal operating potentials, H^+ is the stable form; thus the mechanisms involving H_{ad} require an additional step of the H_{ad} formation from H^+:

$$H^+ + e \rightarrow H_{ad} \quad \text{(step 0)}$$

Assuming an electrode potential of 0.80 V versus SHE leads to ΔE = 0.25 eV for Pt and 0.11 eV for Pd (see Supporting Information). According to Norskov et al.,[13] the enthalpy of step 0 is related to that of

$$H^+ + e \rightarrow 1/2H_2 \rightarrow H_{ad}$$

which is barrierless for SHE.[18] Thus the reaction barrier at an electrode potential of 0.80 V relative to the SHE will likely be close to the reaction enthalpy. Our estimated barrier, 0.25 eV, is consistent with the 0.33 eV calculated by Anderson et al.[18] for Pt. The barriers, 0.25 eV for Pt and 0.11 eV for Pd, are smaller than the RDS barriers for all mechanisms considered in our paper and do not affect our discussions.

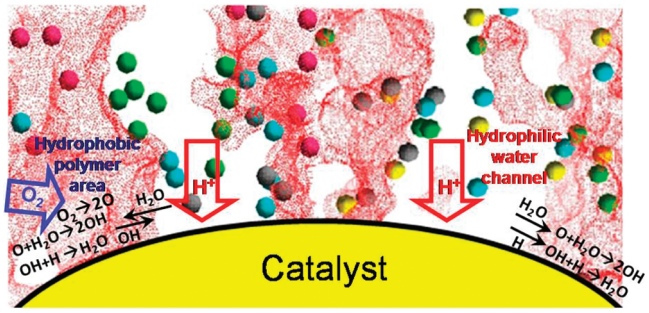

Figure 1. Illustration of the sulfonic acid lined hydrophilic water channels and hydrophobic (Teflon-like) regions in Nafion (from refs 7 and 8) showing the likely locations of the $O_{2\,g} \rightarrow 2O_{ad}$, $O_{ad} + H_2O_{ad} \rightarrow 2OH_{ad}$, and $OH_{ad} + H_{ad} \rightarrow H_2O_{ad}$ steps in the hydrophobic channels, but $H^+ \rightarrow H_{ad}$ at the boundary with the water phase. For the gas phase process, we assume that the proton is chemisorbed on the surface, H_{ad}. For Pt in water at pH = 1 (typical for a fuel cell), this occurs at a potential of −0.06 eV [relative to the standard hydrogen electrode (SHE)].

We report here a new mechanism, **HOO-form-hydr-gas**, for ORR that avoids the high barrier of step 1c or 2d for OH_{ad} formation. This involves hydrolysis of O_{ad} by H_2O_{ad} (step 3d) as an alternative mechanism for forming OH_{ad} from O_{ad}:

$$O_{2g} \rightarrow O_{2ad} \quad \text{(no barrier)} \tag{3a}$$

$$H_{ad} + O_{2ad} \rightarrow HOO_{ad} \quad [E_{act} = 0.30 \text{ eV (Pt)}, 0.55 \text{ (Pd)}] \tag{3b}$$

$$HOO_{ad} \rightarrow HO_{ad} + O_{ad} \quad [E_{act} = 0.12 \text{ eV (Pt)}, 0.26 \text{ (Pd)}] \tag{3c}$$

$$O_{ad} + H_2O_{ad} \rightarrow 2OH_{ad} \quad [E_{act} = 0.23 \text{ eV (Pt)}, 0.30 \text{ (Pd)}] \tag{3d}$$

$$OH_{ad} + H_{ad} \rightarrow H_2O_{ad} \quad [E_{act} = 0.14 \text{ eV (Pt)}, 0.58 \text{ (Pd)}] \tag{3e}$$

Here **HOO-form-hydr-gas** involves HOO formation (E_{act} = 0.30 eV) and then HOO_{ad} dissociation to form O_{ad} and OH_{ad} (E_{act} = 0.12 eV) as in **HOO-form-gas**. However, this is now followed by step 3d, hydration of adsorbed oxygen (E_{act} = 0.23 eV) (Figure 2), and then step 3e (E_{act} = 0.14 eV). Thus step 3b with E_{act} = 0.30 eV is the RDS for Pt versus 0.55 eV for Pd, indicating that Pt is much better.

Table 1

(a) Enthalpies and Barriers (eV) for Steps Possibly Important for ORR on Pt

reaction step barriers Pt	E (gas)	E_{act} (gas)	E (solv)	E_{act} (solv)	E (gas,exp)
O_2 dissociation	−1.23	0.44[a]	−2.18	0.00	0.30[15]
OH formation	−0.32	0.74	−0.07	0.97	
H_2O formation	−0.78	0.14	−0.56	0.24	0.27[16]
OOH formation	−0.24	0.30	−0.19	0.22	
OOH dissociation	−1.30	0.12	−2.07	0.00	
H−OOH dissociation	−1.62	0.14	−2.14	0.00	
O hydration	0.46	0.23	0.49	0.50	0.44[16]

(b) Enthalpies and Barriers (eV) for Steps Possibly Important for ORR on Pd

reaction step barriers Pd	E (gas)	E_{act} (gas)	E (solv)	E_{act} (solv)
O_2 dissociation	−1.02	0.72	−1.91	0.27
OH formation	−0.35	0.30	−0.03	0.47
H_2O formation	−0.59	0.58	−0.39	0.78
OOH formation[b]	0.12	0.55	0.05	0.74
OOH dissociation[b]	−1.49	0.26	−1.99	0.10
H−OOH dissociation[c]	−1.85	0.12	−2.01	0.12
O hydration	0.24	0.30	0.36	0.49

[a] We find a coverage dependence for O_2 dissociation. The barrier is 0.51 eV for $c(2 \times 2)$, 0.45 eV for $c(3 \times 3)$ and 0.44 eV for (4×4) for a three-layer slab. The experimental value is for the limit of zero coverage. [b] The H-associated HOO_{ad} dissociation mechanism is not preferred because of the O_2 dissociation step. [c] Under conditions with high H_{ad}, another mechanism producing HOOH is possible, but this is unlikely under ordinary operating fuel cell conditions. See ref 17.

dx.doi.org/10.1021/jz101753e |J. Phys. Chem. Lett. 2011, 2, 572–576

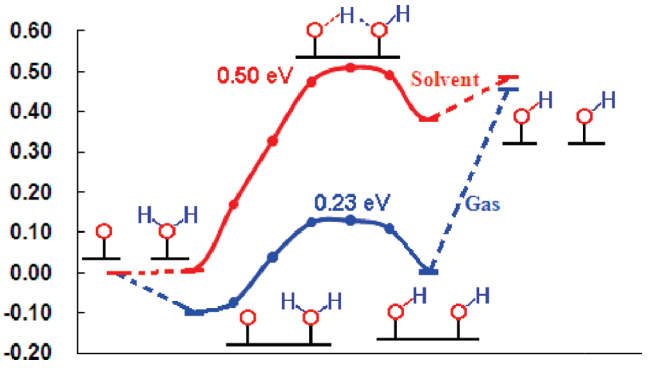

Figure 2. Potential energy surface (eV) for the O_{ad} hydration step of ORR.

Indeed, this O_{ad} hydration step has been observed in experiments by Ertl et al.[16,19] and plays an essential role in the catalytic formation of H_2O at low temperature under ultrahigh vacuum (UHV) conditions. Our calculated barriers are consistent with the Ertl experimental result that H_2O formation ($E_{a,calc}$ = 0.14 eV, $E_{a,exp}$ = 0.27 eV) is much faster than OH formation ($E_{a,calc}$ = 0.23 eV, $E_{a,exp}$ = 0.44 eV). Under UHV conditions, the hydration of O_{ad} becomes impossible at temperatures above 180 K because of the low adsorption energy of water on Pt (calculated 0.21 eV). However, under ORR conditions, there is an abundant supply of water on the surface so that hydration becomes an essential step for ORR. Michaelides and Hu[20,21] using density functional theory (DFT) methods (GGA PW91), found results similar to ours: 0.33 eV for step 3d, 0.21 eV for step 3e, 0.96 eV for step 2d, all 0.1−0.2 eV higher than our results, probably because they used smaller 2 × 2 unit cells and only three- and four-layer slabs instead of the 3×3 unit cell and a six-layer slab in our calculations.

Next we consider how solvation affects the mechanism of ORR using our recently[22] developed approach for estimating the effect of the water phase on these barriers. The contribution of solvation is calculated implicitly using the Poisson−Boltzmann continuum model.[23,24] Including solvation, we find the **O_2 diss-solv** mechanism:

$$O_{2g} \rightarrow O_{2ad} \quad \text{(no barrier)} \tag{4a}$$

$$O_{2ad} \rightarrow 2O_{ad} \quad [E_{act} = 0.00 \text{ eV (Pt)}, 0.27 \text{ (Pd)}] \tag{4b}$$

$$O_{ad} + H_{ad} \rightarrow OH_{ad} \quad [E_{act} = 0.97 \text{ eV (Pt)}, 0.47 \text{ (Pd)}] \tag{4c}$$

$$OH_{ad} + H_{ad} \rightarrow H_2O_{ad} \quad [E_{act} = 0.24 \text{ eV (Pt)}, 0.78 \text{ (Pd)}] \tag{4d}$$

Thus solvation effects dramatically influence the barriers. The O_2 dissociation barrier drops to zero for Pt (0.27 eV for Pd), because of the large solvent stabilization of O_{ad}, increasing the exothermicity from −1.23 eV in gas phase to −2.18 eV in solution for Pt (from −1.02 eV to −1.91 eV for Pd). However, the barrier for OH_{ad} formation (step 4c) increases dramatically from 0.74 to 0.97 eV, making this mechanism unlikely. The reaction of OH_{ad} with H_{ad} to form H_2O is quite favorable with a barrier of 0.24 eV.

In solvent, the **HOO-form-gas** mechanism, involving the formation and dissociation of HOO, becomes the **HOO-form-solv**:

$$H_{ad} + O_{2ad} \rightarrow HOO_{ad} \quad [E_{act} = 0.22 \text{ eV (Pt)}, 0.74 \text{ (Pd)}] \tag{5a}$$

$$HOO_{ad} \rightarrow HO_{ad} + O_{ad} \quad [E_{act} = 0.00 \text{ eV (Pt)}, 0.10 \text{ (Pd)}] \tag{5b}$$

$$O_{ad} + H_{ad} \rightarrow OH_{ad} \quad [E_{act} = 0.97 \text{ eV (Pt)}, 0.47(\text{Pd})] \tag{5c}$$

$$OH_{ad} + H_{ad} \rightarrow H_2O_{ad} \quad [E_{act} = 0.24 \text{ eV (Pt)}, 0.78 \text{ (Pd)}] \tag{5d}$$

Again the RDS becomes OH formation for Pt with a barrier of 0.97 eV and H_2O formation for Pd with a barrier of 0.78 eV. The HOO_{ad} formation barrier is higher than the direct dissociation of O_{2ad}, making it less favorable than the direct O_2 dissociation (step 4b). Thus, we will ignore this mechanism.

In solvent, the barrier for OH formation from step 4c or 5c is 0.97 eV, clearly too high to play an important role at PEMFC operating temperatures. Therefore neither **O_2-diss-solv** nor **HOO-form-solv** is appropriate for Pt in an aqueous environment. Instead we find that **O_2-diss-hydr-solv** is most favorable for solution:

$$O_{2g} \rightarrow O_{2ad} \quad \text{(no barrier)} \tag{6a}$$

$$O_{2ad} \rightarrow 2O_{ad} \quad [E_{act} = 0.00 \text{ eV (Pt)}, 0.27 \text{ (Pd)}] \tag{6b}$$

$$O_{ad} + H_2O_{ad} \rightarrow 2OH_{ad} \quad [E_{act} = 0.50 \text{ eV (Pt)}, 0.49 \text{ (Pd)}] \tag{6c}$$

$$OH_{ad} + H_{ad} \rightarrow H_2O_{ad} \quad [E_{act} = 0.24 \text{ eV (Pt)}, 0.78 \text{ (Pd)}] \tag{6d}$$

Here O hydration (step 5c) is the RDS with a barrier of 0.50 eV for Pt. For Pd the RDS is H_2O formation (step 6d) with a barrier of 0.78 eV, consistent with the decreased performance of Pd. This new mechanism suggests that a strategy for improving efficiency of ORR catalysts is to focus on decreasing the E_{act} for O_{ad} hydration. We have examined this hydration step for 11 metals in columns 8, 9, 10, and 11 of the periodic table and find that the lowest barriers are for Ni (0.20 eV) and Co (0.04 eV), which are already known to increase the efficiency of platinum catalysts.[5,6] We also find low hydration barriers for Os (0.54 eV), Ru (0.69 eV), and Ir (0.69 eV), suggesting that alloying with these elements might also improve the efficiency of Pt cathodes.

The above solvation calculations considered reactions involving H_{ad} formed from H^+ in solution. There might be a direct pathway for H_3O^+ to transfer the H^+ directly to OH_{ad} with a lower barrier than the 0.24 eV we calculate for H_{ad}, but since this is not the RDS, we did not consider this further. Similarly a direct process for $O_{ad} \rightarrow OH_{ad}$ involving H_3O^+ could lower the barrier below the 0.94 eV we find for H_{ad}, but we suspect that the hydration of O_{ad} is still the favorable step. Of course the improved performance for the alloy might arise from other effects, for example, easier OH removal[6] and lower coverage benefiting O_2 dissociation.

The above discussion considered the gas phase and solution phase reactions separately, but the PEMFC allows the O_2 to access the catalyst through the hydrophobic regions of the

dx.doi.org/10.1021/jz101753e |J. Phys. Chem. Lett. 2011, 2, 572–576

Nafion membrane, while the protons to form H_2O arrive through the sulfonic acid lined water channels (illustrated in Figure 1). In this case, the O_{2g} would dissociate to form O_{ad} in the hydrophobic region, which would stay fixed since the barrier for O_{ad} migration is 0.42 eV (Pt). Thus we expect that some H_2O will migrate into this region to form OH_{ad} via the O_{ad} hydrolysis mechanism. However we do not want a full monolayer of H_2O in this hydrophobic region since it would impede O_2 dissociation.

Next we must account for H_2O formation. We assume that the OH_{ad} is formed initially in the hydrophobic region, but since the OH_{ad} migration barrier is <0.1 eV, it can migrate to the part of the Pt in contact with the water channels to react directly with H_3O^+ at the interface. Alternatively, it could remain in the hydrophobic region to react with H_{ad} moving along the surface (barrier only 0.09 eV) from the part of the catalyst in contact with the water channel. A third alternative is that OH in the middle of a monolayer of H_2O in the hydrophobic region could exchange hydrogen ($OH_{ad} + H_2O_{ad} \rightarrow H_2O_{ad} + OH_{ad}$, $E_{act} = 0.03$ eV) to effectively migrate the OH_{ad} to the water channel for reaction with H_3O^+.

Probably the best design would have the O_2 dissociate on the Pt at the interface between hydrophobic and water phases of Nafion so that the O_{ad} could contact H_2O_{ad} to form OH_{ad} on the hydrophobic side but next to the water phase, allowing extraction of the proton from H_3O^+ to form H_2O_{ad}. Thus the optimum membrane for Pt might have the aqueous and hydrophobic phases alternate to maximize the contact length between these phases on the catalysts surface.

COMPUTATIONAL METHODS

In this study, the Pt catalyst particle was modeled as a slab infinite in two directions (a and b) and finite in the third direction (c). We consider a 3 × 3 supercell of the (111) surface (9 atoms) that is six layers thick (54 atoms). The top two layers are allowed to relax, representing the active surface, while the bottom four layers are fixed, representing the bulk side of the surface. The same model was applied in previous studies.[22]

All calculations employed the kinetic and exchange-correlation functional developed by Perdew, Burke and Ernzerhof (PBE).[25] We used the SeqQuest[26] implementation with an optimized double-ζ plus polarization Gaussian type basis set contracted from calculations on the most stable unit cell of the pure elements. Angular-momentum-projected norm-conserving nonlocal effective core potentials[27−30] (pseudopotentials) were used to replace the core electrons. Thus, the Pt atom was described with 16 explicit electrons (six 5p, one 6s, and nine 5d in the ground state). The real space grid density was 5 points/Å, while the reciprocal space grid was 5 × 5 × 0 for slab calculations. All calculations allowed the up-spin orbitals to be optimized independently of the down spin orbitals (spin-unrestricted DFT).

The solvation of the water phase employed a continuum model based on the Poisson−Boltzmann approximation.[23,24,31,32] All reaction pathways were determined using the Nudged Elastic Band[33,34] method, and solvent effects were included for each point along the path.

ASSOCIATED CONTENT

Supporting Information. $H^+ \Leftrightarrow H_{ad}$ reaction barriers and the availability of H_{ad} on the surface. This material is available free of charge via the Internet http://pubs.acs.org.

AUTHOR INFORMATION

Corresponding Author
*E-mail: wag@wag.caltech.edu.

ACKNOWLEDGMENT

This research was supported partially with funding from the Ford Motor Company and from the DOE (DE-AC02-06CH11357). We thank Dr. Gerald Voecks for helpful discussions.

REFERENCES

(1) Kordesch, K.; Simader, G. *Fuel Cells and Their Applications*; VCH: New York, 1996.
(2) Appleby, A.; Foulkes, F. *Fuel Cell Handbook*; Van Nostrand Reinhold: New York, 1989.
(3) Brandon, N. P.; Skinner, S.; Steele, B. C. H. Recent Advances in Materials for Fuel Cells. *Annu. Rev. Mater. Res.* **2003**, *33*, 183–213.
(4) Mehta, V.; Cooper, J. S. Review and Analysis of PEM Fuel Cell Design and Manufacturing. *J. Power Sources* **2003**, *114*, 32–53.
(5) Beard, B. C.; Ross, P. N. The Structure and Activity of Pt−Co Alloys as Oxygen Reduction Electrocatalysts. *J. Electrochem. Soc.* **1990**, *137*, 3368–3374.
(6) Stamenkovic, V. R.; Fowler, B.; Mun, B. S.; Wang, G. F.; Ross, P. N.; Lucas, C. A.; Markovic, N. M. Improved Oxygen Reduction Activity on $Pt_3Ni(111)$ via Increased Surface Site Availability. *Science* **2007**, *315*, 493–497.
(7) Jang, S. S.; Molinero, V.; Cagin, T.; Goddard, W. A. Nanophase-Segregation and Transport in Nafion 117 from Molecular Dynamics Simulations: Effect of Monomeric Sequence. *J. Phys. Chem. B* **2004**, *108*, 3149–3157.
(8) Jang, S. S.; Molinero, V.; Cagin, T.; Goddard, W. A. Effect of Monomeric Sequence on Nanostructure and Water Dynamics in Nafion 117. *Solid State Ionics* **2004**, *175*, 805–808.
(9) Jacob, T.; Goddard, W. A. Water Formation on Pt and Pt-Based Alloys: A Theoretical Description of a Catalytic Reaction. *ChemPhysChem* **2006**, *7*, 992–1005.
(10) Hyman, M. P.; Medlin, J. W. Theoretical Study of the Adsorption and Dissociation of Oxygen on Pt(111) in the Presence of Homogeneous Electric Fields. *J. Phys. Chem. B* **2005**, *109*, 6304–6310.
(11) Janik, M. J.; Taylor, C. D.; Neurock, M. First-Principles Analysis of the Initial Electroreduction Steps of Oxygen over Pt(111). *J. Electrochem. Soc.* **2009**, *156*, B126–B135.
(12) Wang, Y.; Balbuena, P. Ab Initio Molecular Dynamics Simulations of the Oxygen Reduction Reaction on a Pt (111) Surface in the Presence of Hydrated Hydronium $(H_3O)^+(H_2O)_2$: Direct or Series Pathway?. *J. Phys. Chem. B* **2005**, *109*, 14896–14907.
(13) Norskov, J. K.; Rossmeisl, J.; Logadottir, A.; Lindqvist, L.; Kitchin, J. R.; Bligaard, T.; Jonsson, H. Origin of the Overpotential for Oxygen Reduction at a Fuel-Cell Cathode. *J. Phys. Chem. B* **2004**, *108*, 17886–17892.
(14) Ford, D. C.; Nilekar, A. U.; Xu, Y.; Mavrikakis, M. Partial and Complete Reduction of O_2 by Hydrogen on Transition Metal Surfaces. *Surf. Sci.* **2010**, *604*, 1565–1575.
(15) Gland, J. L.; Sexton, B. A.; Fisher, G. B. Oxygen Interactions with the Pt(111) Surface. *Surf. Sci.* **1980**, *95*, 587–602.
(16) Sachs, C.; Hildebrand, M.; Volkening, S.; Wintterlin, J.; Ertl, G. Reaction Fronts in the Oxidation of Hydrogen on Pt(111): Scanning Tunneling Microscopy Experiments and Reaction-Diffusion Modeling. *J. Chem. Phys.* **2002**, *116*, 5759–5773.
(17) When hydrogen is present, it can react with surface HOO_{ad} to form two HO_{ad}, leading to a barrier of 0.14 eV in gas phase. Combining this step with the formation of HOO leads to the **HighH-gas** mechanism:

$$O_{2g} \rightarrow O_{2ad} \quad \text{(no barrier)} \qquad (7a)$$

$$H_{ad} + O_{2ad} \rightarrow HOO_{ad} \quad [E_{act} = 0.30 \text{ eV (Pt)}, 0.55 \text{ (Pd)}] \qquad (7b)$$

$$H_{ad} + HOO_{ad} \rightarrow 2HO_{ad} \quad [E_{act} = 0.14 \text{ eV (Pt)}, 0.12 \text{ (Pd)}] \qquad (7c)$$

$$OH_{ad} + H_{ad} \rightarrow H_2O_{ad} \quad [E_{act} = 0.14 \text{ eV (Pt)}, 0.58 \text{ (Pd)}] \qquad (7d)$$

Here the RDS is HOO formation for both gas phase and solvent with E_a = 0.30 eV. This mechanism might be favorable only under extremely high coverage of H_{ad}, since the barrier for 7c ($H_{ad} + HOO_{ad}$) is higher than that for 3c (HOO_{ad} dissociation). In operating fuel cells, it is not likely to have such a high H_{ad} coverage.

(18) Anderson, A. B.; Sidik, R. A.; Narayanasamy, J.; Shiller, P. Theoretical Calculation of Activation Energies for Pt + H^+(aq) + $e^{(-)}$(U) ⟷ Pt−H: Activation Energy-Based Symmetry Factors in the Marcus Normal and Inverted Regions. *J. Phys. Chem. B* **2003**, *107*, 4618–4623.

(19) Völkening, S.; Bedürftig, K.; Jacobi, K.; Wintterlin, J.; Ertl, G. Dual-Path Mechanism for Catalytic Oxidation of Hydrogen on Platinum Surfaces. *Phys. Rev. Lett.* **1999**, *83*, 2672–2675.

(20) Michaelides, A.; Hu, P. Catalytic Water Formation on Platinum: A First-Principles Study. *J. Am. Chem. Soc.* **2001**, *123*, 4235–4242.

(21) Michaelides, A.; Hu, P. A Density Functional Theory Study of Hydroxyl and the Intermediate in the Water Formation Reaction on Pt. *J. Chem. Phys.* **2001**, *114*, 513–519.

(22) Sha, Y.; Yu, T. H.; Liu, Y.; Merinov, B. V.; Goddard, W. A. Theoretical Study of Solvent Effects on the Platinum-Catalyzed Oxygen Reduction Reaction. *J. Phys. Chem. Lett.* **2010**, *1*, 856–861.

(23) Tomasi, J.; Persico, M. Molecular Interactions in Solution: An Overview of Methods Based on Continuous Distributions of the Solvent. *Chem. Rev.* **1994**, *94*, 2027–2094.

(24) Cramer, C.; Truhlar, D. Implicit Solvation Models: Equilibria, Structure, Spectra, and Dynamics. *Chem. Rev.* **1999**, *99*, 2161–2200.

(25) Perdew, J.; Burke, K.; Ernzerhof, M. Generalized Gradient Approximation Made Simple. *Phys. Rev. Lett.* **1996**, *77*, 3865–3868.

(26) Schultz, P. SeqQuest code project; Sandia National Laboratories: Albuquerque, NM (http://www.cs.sandia.gov/~paschul/Quest/).

(27) Melius, C. F.; Goddard, W. A. Ab-Initio Effective Potentials for Use in Molecular Quantum-Mechanics. *Phys. Rev. A* **1974**, *10*, 1528–1540.

(28) Melius, C. F.; Olafson, B. D.; Goddard, W. A. Fe and Ni Ab-Initio Effective Potentials for Use in Molecular Calculations. *Chem. Phys. Lett.* **1974**, *28*, 457–462.

(29) Redondo, A.; Goddard, W. A.; Mcgill, T. C. Ab Initio Effective Potentials for Silicon. *Phys. Rev. B* **1977**, *15*, 5038–5048.

(30) Hamann, D. R. Generalized Norm-Conserving Pseudopotentials. *Phys. Rev. B* **1989**, *40*, 2980.

(31) Tannor, D. J.; Marten, B.; Murphy, R.; Friesner, R. A.; Sitkoff, D.; Nicholls, A.; Ringnalda, M.; Goddard, W. A.; Honig, B. Accurate First Principles Calculation of Molecular Charge-Distributions and Solvation Energies from Ab-Initio Quantum-Mechanics and Continuum Dielectric Theory. *J. Am. Chem. Soc.* **1994**, *116*, 11875–11882.

(32) Baker, N.; Sept, D.; Joseph, S.; Holst, M.; McCammon, J. Electrostatics of Nanosystems: Application to Microtubules and the Ribosome. *Proc. Natl. Acad. Sci. U.S.A.* **2001**, 181342398.

(33) Mills, G.; Jonsson, H.; Schenter, G. K. Reversible Work Transition-State Theory - Application to Dissociative Adsorption of Hydrogen. *Surf. Sci.* **1995**, *324*, 305–337.

(34) Mills, G.; Jonsson, H. Quantum and Thermal Effects in H_2 Dissociative Adsorption - Evaluation of Free-Energy Barriers in Multidimensional Quantum-Systems. *Phys. Rev. Lett.* **1994**, *72*, 1124–1127.